

1 This is a non-peer reviewed case study submitted to EarthArXiv

2

3 Exploring Foundation Models for Seismic Event Processing

4

5 Lisa Linville

6 Sandia National Laboratory

7 1515 Eubank Blvd. SE

8 MS 0401

9 Albuquerque, NM 87123

10 llinvil@sandia.gov

11

12

13 Abstract

14

15 Nonproliferation monitoring efforts benefit from a glut of multi-modal data that related research  
16 must develop methods to process efficiently. Many of the highest performing methods for  
17 predictive modeling rely on a legacy of data curation and labeling that is available from decades  
18 of seismic catalog building but may not scale well for future uses. This work explores tools for  
19 predictive modeling with unlabeled datasets. Unlike clustering methods, which have outcomes  
20 that may not be dominated by phenomenologies of interest, self-supervised learning uses an  
21 objective function to direct attention to signal attributes that matter for predictive learning. The  
22 models developed in this work are patterned after breakthroughs in natural language processing  
23 and the work borrows two training methods from large language models adapted to the seismic  
24 domain. The first objective is a fill in the blank task where parts of the signal are masked, and the  
25 model learns to accurately predict missing values. The second objective is a classification task  
26 where a model must learn when two observations were generated by the same source (event).  
27 Model training with these two objectives results in a base model with contextual knowledge of  
28 characteristic event sequences. The base models are then used with various quantities of labeled  
29 data on the task of event discrimination. Classification performance is competitive with existing  
30 methods but does not reach state of the art. Temporal sequence modeling provides most of the  
31 performance while adding contextual knowledge augments performance by 1-3%. Evaluation of

32 the learned representations suggests that knowledge encoding fits domain expectations and  
33 future work should focus on adaptations to reduce complexity in the training pipeline and on the  
34 potential use of learned representations for event discrimination.

35

36 Background

37

38 Currently much or all deep learning exploration in seismic event processing involves raw or  
39 minimally transformed data as model input. One specific reason deep learning is attractive is the  
40 expectation of optimal feature learning with respect to a specific task. Feature learning is  
41 assumed to be optimized because it is tightly coupled with predictive model building. Using  
42 waveform or spectrogram data minimizes expectations and inductive bias assertions that may not  
43 always result in the best predictive performance, even when they are intuitive for a specific  
44 domain. For example, when we know that p/s spectral ratios and time-of-day information are  
45 important for explosive source identification, using these attributes directly enables the use of  
46 models that are simple and have dependencies and mechanics that are more transparent. For  
47 constrained problems where limited generalization is required, this approach may be sufficient  
48 (Rudin, 2019). By comparison, the deep neural network (DNN) approach expects a model to  
49 learn attributes that are useful for enhancing performance directly from the data but become  
50 difficult to understand causally. Currently, DNN methods have proven to be powerful and  
51 transformative in seismology for seismic event processing specifically on account of decades of  
52 investments in monitoring and observation that have resulted in informative and accurate labeled  
53 data in abundance. When the predictive capability of DNN models far surpasses simple models  
54 built on interpretable features, the future research directions necessarily shift to understanding  
55 what the boundaries on DNN model use are. For example, how to manipulate architectures and  
56 inference methods that give us a sense of the uncertainty on model predictions, or how to access  
57 the internal and intermediate representations that help us build intuition for how to believe, trust,  
58 and defend model decisions. These are important avenues of research that are needed to help  
59 bridge knowledge gaps between performance gains proven by machine learning research and  
60 practical applications at scale within current processing systems.

61

62 While labeled (supervised) learning research meets many near-term goals for advancing the  
 63 current state of seismic event processing pipelines, exploration of methods that address the  
 64 shortcomings of labeled deep learning in the face of expanding data landscapes and the need for  
 65 information integration across dataspace, domains, and tasks are increasing in importance for  
 66 intermediate to long-term goals. Learning highly informative representations from unlabeled data  
 67 may therefore be an important avenue for data modeling moving forward. This work explores  
 68 representation learning as a foundation for a broad range of tasks in seismology that could  
 69 benefit from the context available outside of specific labeled attributes. For example, models  
 70 with an inherent understanding of temporal signal patterns from earthquakes observed at various  
 71 scales may be helpful when those models are subsequently trained to predict onset times, event  
 72 durations, and other related attributes. The analog for temporal signal learning in seismology as  
 73 proposed in this work is self-training as realized in natural language processing, which has  
 74 fundamentally changed the capabilities in that field.

75

76 *Table 1. Reasons for transformative potential with self-supervised learning in the seismic*  
 77 *domain.*

| Reasons self-supervised representation learning could be transformative in seismic event processing   |
|---|
| Eliminates the need to train models bottom up for each task. Saves resources (power, time), minimizes engineering burden associated with experiment setup, standardizes input, increases accessibility to model building for non-experts. |
| Potential for increased performance and dataset integration. Fine-tuning (or transfer learning from base models) allows the efficient use of disparate datasets.  |
| Encourages exploratory rather than prescriptive learning for seismic representations which could be vital for new knowledge discovery and introspection.  |
| Expands the usability of the dataspace beyond labeled ground truth.   |

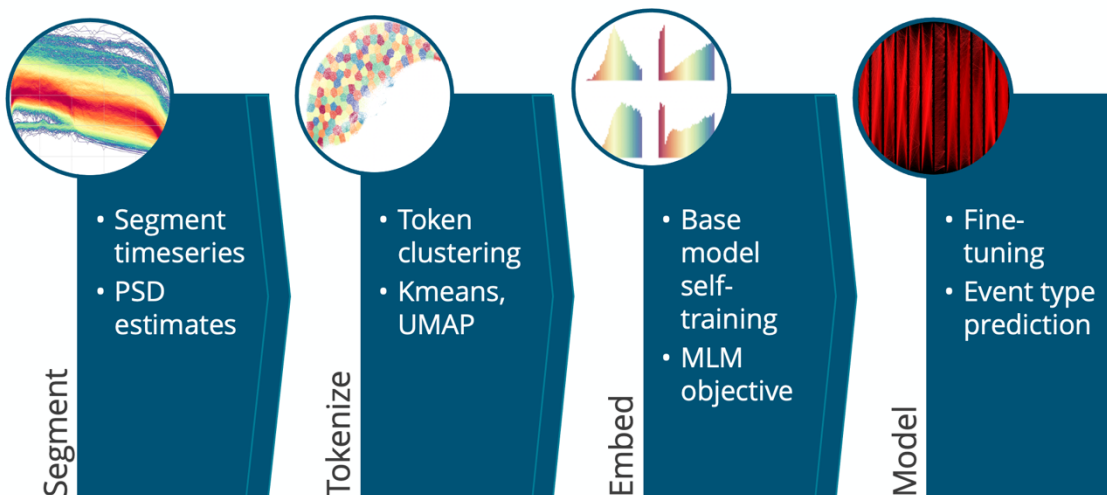
78

79

80 Method

81

82 The paradigm this work is patterned off relies on large text datasets that are translated into  
 83 discrete numerical representations called tokens. The tokens are then used to train foundation  
 84 models (Lacoste et al., 2021; Horawalavithana et al., 2022) on a range of tasks. Similarly, this  
 85 work relies on a corpus of examples transformed through a series of steps. The **segmentation**  
 86 process discretizes continuous waveforms into temporally discrete windows. The **tokenization**  
 87 process maps the segmented data into a finite set of states akin to a vocabulary. Context specific  
 88 representations are then built by observing the structure of the vocabulary over the duration of an  
 89 event in the **pretraining** phase. Final **fine-tuning** for specific tasks then occurs with respect to  
 90 the context learned over the vocabulary. The 4 processes (segmentation, tokenization,  
 91 embedding, and modeling) that comprise the pipeline for developing a Bert-style model (Devlin  
 92 et al., 2018) for seismic event processing (SeisBert) are shown in Figure 1.  
 93

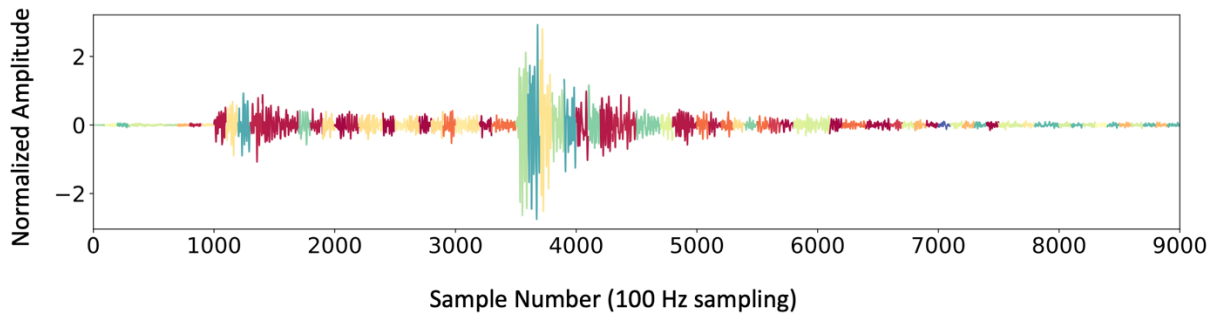


94  
 95 *Figure 1. SeisBert Pipeline*

96  
 97 **Segmentation**

98  
 99 Although a long-range goal is to use the proposed method to process continuous seismic data,  
 100 this work constrains the dataspace to times during which a seismic event has been previously  
 101 identified. This study uses only event-based waveforms where continuous seismic records are  
 102 segmented to window discrete known seismogenic phenomena, specifically earthquakes and  
 103 quarry blasts.

104



105

106

107 *Figure 2. Event-based waveform for a single example. Raw waveforms are segmented into 1sec*  
108 *data windows and colored based on clustering results (see clustering section). Although this*  
109 *method is appealing for overall simplicity, practical application at scale requires an additional*  
110 *dimensionality reduction step that increases the complexity, computational burden, and reduces*  
111 *the interpretability without comparative benefits on performance.*

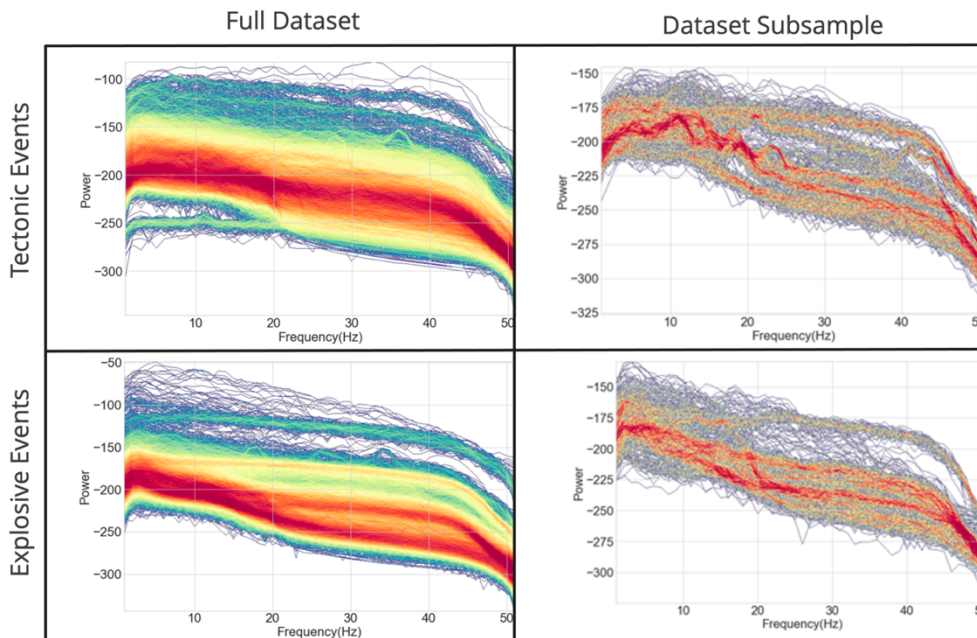
112

113 In the past, time-frequency representations (spectrograms or continuous wavelet transforms-  
114 CWT) have been identified as being highly informative representations that result in efficient  
115 learning with DNN models compared with raw waveforms. Both time-frequency and waveform  
116 representations were explored based on their impact on downstream processes. While raw  
117 waveforms are attractive for the minimal preprocessing they require, the interpretability of the  
118 resulting ‘states’ (windowed parts of an event), and their inherent scaling after high-pass filtering  
119 (centered on zero), they did not prove to be as usable for reasons discussed in the tokenization  
120 section. Therefore, while tokenization of raw waveforms (Figure 2) or skipping the tokenization  
121 process entirely are ongoing research topics, the rest of this work focuses on exploration using  
122 time-frequency (specifically spectrogram) representations of the data.

123

124 This work relies on 1-2sec power spectral density (PSD) estimates over the duration of a seismic  
125 event starting 10 sec prior to the first arriving energy and lasting 80 sec following the first arrival  
126 on data sampled at 100 Hz. For an individual event there will be 45 (in the case of 2 sec  
127 windows) or 90 (in the case of 1 sec windows) individual PSD estimates. Although 3 channel  
128 (vertical, radial, transverse) seismic events were explored, the results and analysis rely on the 90

129 1 sec PSD estimates for vertical channels only. The PSD estimates have a frequency resolution  
 130 of 1hz and the frequencies retained range of 1-20Hz for total of 20 frequency features at 90  
 131 independent times (no overlap). A dataset with 5 events, where each event was observed on 5  
 132 stations would result in 2.25k PSD examples ( $5*5*90$ ) or a data array with the shape (25,90,20).  
 133 The dataset used in this work comes from previous work on events compiled from the University  
 134 of Utah (Linville et al., 2019; Linville, 2022) and uses a total of 15,282,720 PSD estimates  
 135 (169808, 90, 20).  
 136  
 137 Scaling is usually an important data processing step that helps keep weights in a DNN centered  
 138 on zero for more stable learning (Narkhede et al., 2022). In this work no scaling, a min/max  
 139 scaling, and event-level whitening, and a median normalization approach were explored.  
 140 Minimal differences were observed across the normalization methods and the analysis and  
 141 results reported here rely on PSD estimates divided by the signal median for each frequency bin.



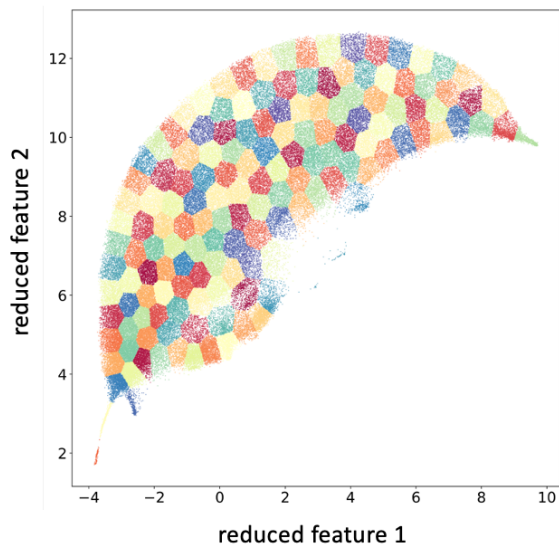
142

*Figure 3. Differences between PSD collections for explosive and tectonic events. Vertical channel power spectral density (PSD) estimates for 2sec windows over earthquake (top) and explosive (bottom) waveforms compared to less dense sampling of just a few events compared to hundreds (right). The differences in character justify exploration of discrimination based on the temporal variation in PSD estimates.*

143 Tokenization

144

145 Tokenization in natural language processing (NLP) breaks down text into a base constituency  
146 (word or subword level) that is combinatorially complete, yet retains more context than  
147 individual characters. The minimal number of tokens in a text corpus represents the vocabulary.  
148 In most cases, the vocabulary that foundational models are trained over is large (models used in  
149 industry for example such as GPT and GPT-2 have vocabularies of 40,478 and 50,257  
150 respectively). Unlike the discrete alphabets and symbologies that comprise language across text  
151 and audio modalities, seismic data is generated by a continuous system. Decomposing audio into  
152 its constituent language parts (audio tokenization) discards information about the carrier, the  
153 emotional state, and many other phenomenologies that influence signal character. It may be  
154 valuable to remove speaker, emotional state, microphone response, etc. from an audio signal  
155 when source generating mechanics are the fundamental interest, but requiring audio  
156 representations to mirror text, or to be predictive as text is, can minimize the impact of the  
157 unique information the modality brings to bear. For example, shouting can change the sound and  
158 consequently the numerical mapping of a part of speech. It might not change the token, even  
159 when it changes the meaning. Token level ambiguity is part of why context from temporal  
160 sequences becomes vital compared to static embeddings such as Word2Vec (Mikolov et al.,  
161 2017). In the absence of diagnostic information from the immediate state, we turn to longer  
162 range context from a scenario as it unfolds over time, and this is likely why attention  
163 mechanisms have become a critical part of sequence processing. This work adheres to the single-  
164 modality tokenization paradigm of existing NLP models for the sake of knowledge building  
165 across these two application spaces.



167

168 *Figure 4. PSD features reduced to 2D and colored by cluster value. The colors show the k-means*  
 169 *results. In the absence of user-defined clusters there is no clear way to segment data clouds with*  
 170 *homogeneous density using methods such as DBSCAN. We observe similar behaviors when*  
 171 *reducing waveform data directly.*

172 K-means (Pedregosa et al., 2011; Seinley, 2006) is one of the most straightforward ways to  
 173 identify clusters within a dataspace but one drawback of using K-means is that the number of  
 174 clusters must be specified. Methods that automatically identify and determine the number of  
 175 clusters have been developed such as DBSCAN (Khan et al, 2014; Pedregosa et al., 2011) and  
 176 are attractive in the absence of knowledge regarding the expected scale, size, and content of a  
 177 seismic vocabulary. However, low-dimensional remapping of the seismic data sets and iterative  
 178 testing under various parameterizations suggests that samples fall within a continuum where  
 179 segmentation rather than clustering is appropriate. For example, Figure 4 shows a lack of discrete  
 180 clusters in the 2D remapping of PSD values within the training partition (80% of samples). The  
 181 propensity for data samples to fall within a single majority cluster implies that the topology  
 182 visualized in 2D space persists in higher dimensions. Therefore, categorizing PSD values  
 183 according to their ‘differences’ requires the explicit specification of the number of expected or  
 184 desired clusters (colors in Figure 4), making K-means a reasonable approach.

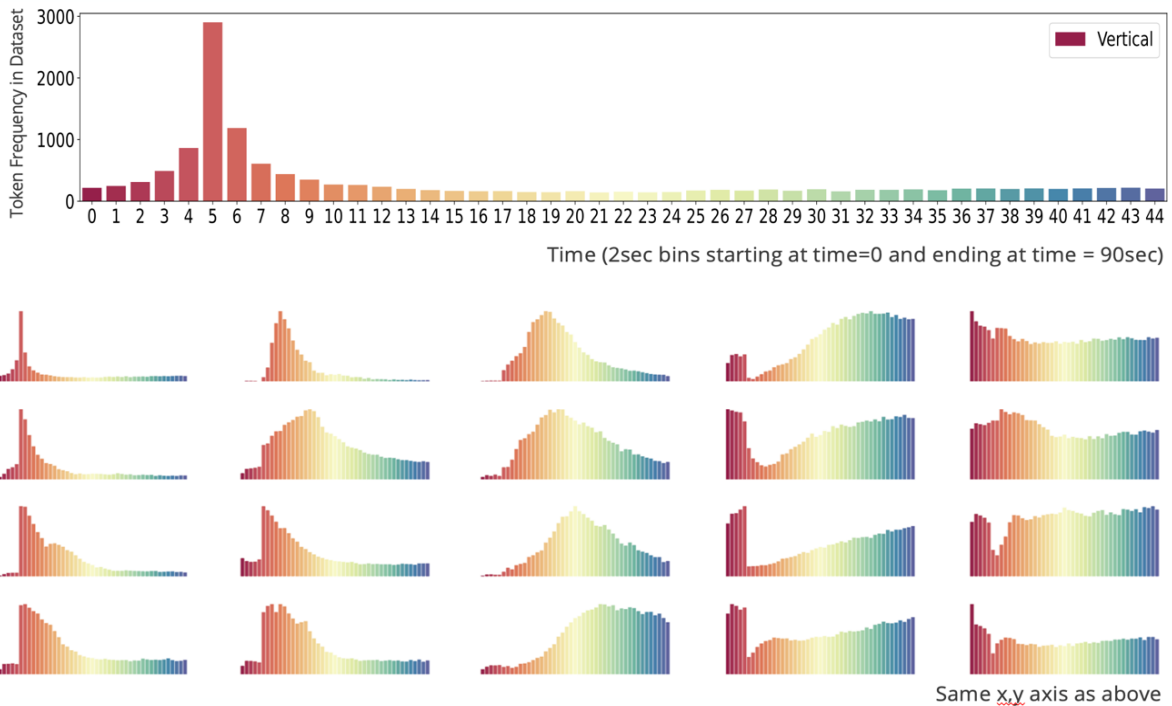
185

186 K-means on raw waveforms results in one or few dominant clusters, while K-means on  
187 dimensionally reduced waveforms discretized into 1 second intervals (McInnes et al., 2018)  
188 leads to the same cluster characteristics available through K-means performed directly on PSD  
189 estimates. For simplicity, this work performs clustering on PSD estimates. The temporal  
190 evolution of “states” related to source processes (for example: event onset, discrete wave phases,  
191 coda) are expected to be significantly less abundant than language vocabularies; this is the  
192 primary assumption driving the assigned number of clusters. The largest number of clusters  
193 tested was 150 and the minimum number was 8. Analysis in this work is focused on modeling  
194 with 150 tokens (clusters). For any 1 second of arriving energy during an event, the model has  
195 150 options to describe the characteristic signal at that time.

196  
197 The discretization of continuous waveform data into PSD estimates and subsequently tokens is  
198 one of many possible ways to leverage the context available in this domain. There are other  
199 frameworks worth mentioning which are left largely unexplored in this work. One main  
200 alternative to foundation models and subsequent fine-tuning is to develop word vector  
201 representations (wave2vec; Mikolov et al., 2017). Static embeddings with models like wave2vec  
202 may potentially be attractive future methods in non-proliferation monitoring if the range of use  
203 cases and the probability of their occurrences can be meaningfully encoded in a static  
204 representation that prove to be adequate for down-stream tasks.

205  
206 The primary method of evaluating the effectiveness of a clustering approach is the impact it has  
207 on downstream learning, which is discussed in the modeling section. Another indirect approach  
208 is to observe how often a token occurs, and when, over the duration of a seismic event observed  
209 on an individual sensor (Figure 5). The tokens developed through k-means clustering of 1 sec  
210 PSD estimates reflect states that occur over the duration of a seismic event. For example, some  
211 tokens are most commonly sensitive to first arrivals, pre-event background, or coda and scattered  
212 energy. This analysis suggest that tokens may link to domain phenomenologies such as P-wave,

213 S-wave, ambient, and coda wave energy. It also suggests that the number of states may be over-  
214 represented in a vocabulary of this size (150 tokens).



215  
216 *Figure 5. Frequency of occurrence for individual tokens over the duration of a seismic event.*  
217 *Out of 150 tokens there are broadly 6-8 categorizations for how each token is observed over the*  
218 *duration of an event. In this figure 20 tokens are chosen out of the full vocabulary and organized*  
219 *in columns according to their similarity. For example, the 4 tokens in the fourth column from the*  
220 *left show that they are all highly sensitive to the pre-event noise and insensitive to first arrival*  
221 *characteristics.*

222  
223 Embedding: pretraining (with masked language modeling and source linking)

224  
225 The premise of successful self-supervised learning is that structure in a dataset provides powerful  
226 context for what a model understands when making observations. The success of model learning  
227 requires objectives capable of providing useful constraints. Masked language modeling (MLM)  
228 is one common objective used in bidirectional sequence modeling. The expectation is that if a  
229 model can correctly predict missing words within a sentence, it will do so successfully by

230 learning to understanding basic rules of grammar and syntax and using context clues from the  
231 surrounding text. Translated to the seismic domain, that would suggest that applying token  
232 masking and requiring the model to ‘fill in the blank’ forces a model to develop an understanding  
233 of the typical structure of a seismic event sequence, in essence an understanding of where a 1 sec  
234 data example is likely to belong within an event sequence. The idea is that this learned ‘context’  
235 is subsequently helpful when a model is asked to perform a specific task such as p-wave  
236 identification or event classification.

237

238 There are other common self-supervised objectives such as next word prediction or next sentence  
239 prediction (NSP). Directly applied to the seismic learning NSP could look like mix-match  
240 sampling for the first and second half of an event sequence. NSP in this work is applied as a  
241 source forcing identifier across stations that observe a specific event. If the first half of a token  
242 sequence comes from a different event than the second half, the model is required to recognize  
243 this state as different from when the first and second half come from the same event but different  
244 stations. The labels associated with NSP in this case designate where in the sequence the data  
245 origin changes and whether that origin change is from a new event, or a new station from the  
246 same event. The sequence label is 45 characters that take on values between 0 and 1. The NSP  
247 label is then binary depending on if all 45 tokens share a source (0) or not (1).

248

249 The most effective self-supervised learning objectives may be domain and task specific and  
250 assessing their value is currently quantified indirectly through model performance on  
251 downstream tasks. This work utilizes MLM and MLM+NSP for base model building. The DNN  
252 model architecture uses the transformer architecture (Vaswani et al., 2017). Transformers have  
253 recently supplanted Long-Short-Term-Memory networks, providing the same sequence modeling  
254 objectives which higher computational efficiency (e.g., parallelization of sequence processing).  
255 A common NLP model architecture that utilizes both forward and backward sequence modeling  
256 is the Bidirectional Encoder Representations for Transformers or BERT models (Devlin et al,  
257 2018). This work tests BERT models with variations in model complexity and capacity (the  
258 number of attention heads and the depth, or number of layers) on a small event-based dataset  
259 (~10k events).

260

261

262 Model: finetuning

263

264 To limit the engineering complexity of this pilot investigation the modeling task is constrained to  
265 be binary event type classification. In the process of finetuning a model we take as input the  
266 segmented, tokenized, embedded data and the trained base model, and then use labels to learn a  
267 classification network that can successfully discriminate tectonic from explosive sources. None  
268 of the layers are fixed during finetuning, meaning the encoding layers of the model can change  
269 according to how adeptly they lead to successful classification. In this work base models are  
270 trained with the MLM objective, the MLM and NSP objectives jointly. Models with the same  
271 architecture and no base training are also tested to evaluate how much impact representation  
272 learning at this scale has on model performance for the discrimination task.

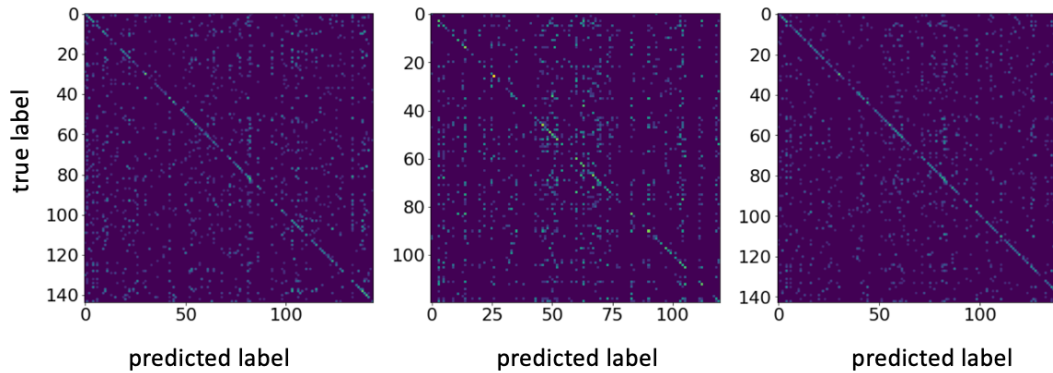
273

274

275 Results

276

277 During pretraining the point of self-supervised training is to learn valuable data representations  
278 and relationships. The ultimate metric of successful representation learning is how well it  
279 enhances performance on a model fine-tuned for downstream tasks, in this case binary  
280 classification. However, metrics over pretraining are needed to select, with validation data,  
281 which models to use in subsequent finetuning trials. Here the multiclass accuracy score on  
282 masked tokens is used. Only the models that perform the best on filling in the blanks (MLM) go  
283 on to train with labels. Models rarely achieve scores that perform better than 30% across all  
284 tokens. Although this leaves room for improvement, the values are considerably better than  
285 random guessing (0.6%) or using the average token per time step from the training data (1.1%  
286 accuracy). Visualization for what 30% accuracy looks like on a 150-class problem is shown in  
287 Figure 6. Perfect prediction would result in the brightest colors along the diagonal only with blue  
288 background elsewhere.

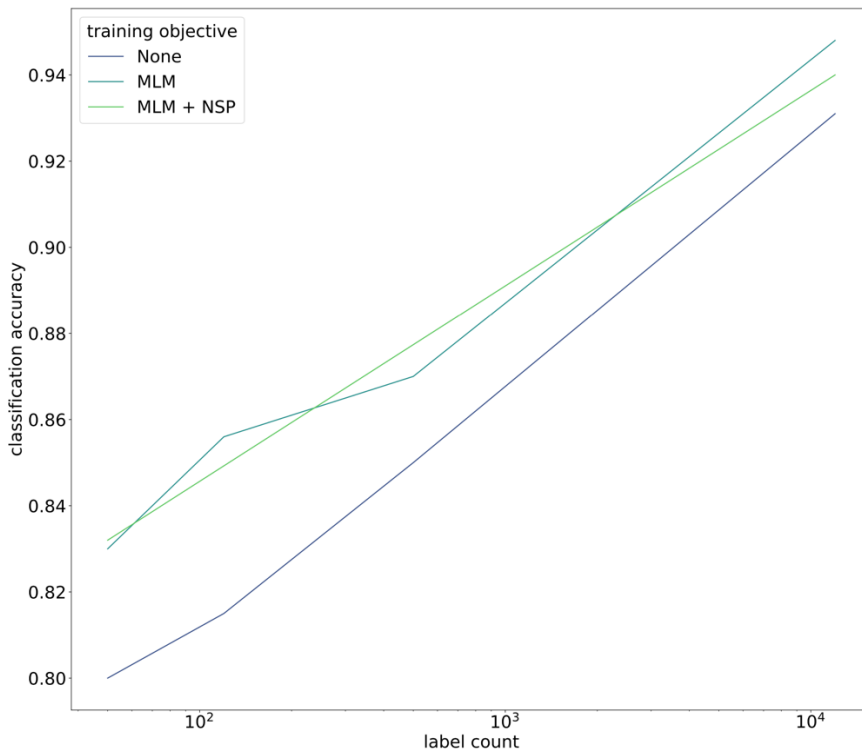


289

290 *Figure 6. Confusion matrix for prediction on the second half of the signal when the first half is*  
 291 *masked (left), predictions on the first half when the second half is masked (middle), and*  
 292 *predictions for random signal locations masked events (right).*

293 Classification performance reaches 95% and is highest with the largest base models (12 heads  
 294 per layer, 12 layers). MLM and MLM+NSP base models perform similarly. Although typically  
 295 this would be an indictment of NSP as being unhelpful for source prediction, the performance of  
 296 both MLM and NSP models continues to increase together with increasing model size (number  
 297 of heads and number of layers), an indication that model performance for both training  
 298 objectives may be architecture limited at the least, and potentially both data and architecture  
 299 limited. Masking the first half of the input reduces event type prediction to 66.6%, increasing to  
 300 70.3% when masking the second half and 86.4% for random (76% masking). If all tokens are  
 301 masked the model always predicts the positive class (quarry blast).

302



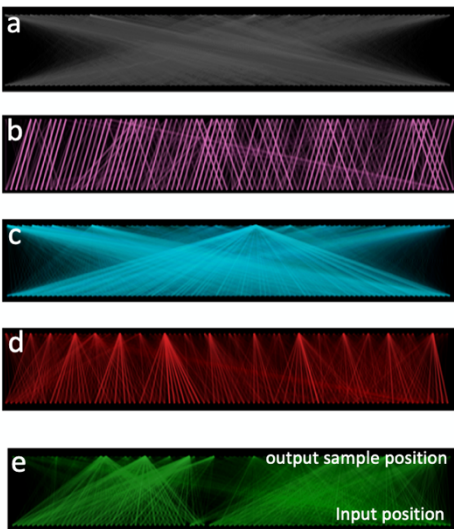
303  
 304 *Figure 7. Classification accuracy given a set of randomly sampled event labels. Sample sizes are*  
 305 *50, 120, 500 and the entire dataset. Note there is only data for the first and last label counts for*  
 306 *the MLM + NSP objective.*

307  
 308 Information about what the models learn to pay attention to can provide insight regarding what  
 309 kind of information the model uses for context and decision making. Figure 8 shows how  
 310 different attention heads in different layers learn to allocate attention in similar ways as receptive  
 311 fields with variable kernel sizes in common computer vision processing models (convolution  
 312 neural networks). Similarly, the attention strength across different heads within a single layer  
 313 shows that the model has developed filters that attend to nearly all aspects of the signal with  
 314 variable overlap and strength, and that these regions of importance change according to where  
 315 your prediction target is within the example. Figure 9 shows what layer 7 of 12 passes to layer 8  
 316 in terms of signal weighting from each head with respect to the 15<sup>th</sup> token in the sequence of this  
 317 input example. While various heads attend to different portions of the waveform, there are some  
 318 heads that dominate signal importance. Figure 9 is meant to convey intuition for the  
 319 comprehensive piecewise attention coverage across the waveform and illuminate the differences

320 in receptive field and weight complexity. The model is of sufficient depth that attention heads  
321 across various layers can become specialized without excessive redundancy (because these  
322 attention filters respond differently from each other given a new input). A more easily  
323 interpretable summary of what a model responds to may be gained by a summation of the  
324 attention over all heads and layers. In this case, we get a sense of which parts of the waveform  
325 for a specific input are most important for prediction at a specific point in the event sequence  
326 overall (Figure 10). A catalog of animations over the progression of an event highlights that 1)  
327 learned attention makes physical sense and 2) there is an abundance of information available to  
328 exploit in understanding statistical event classification for this catalog of signals.

329

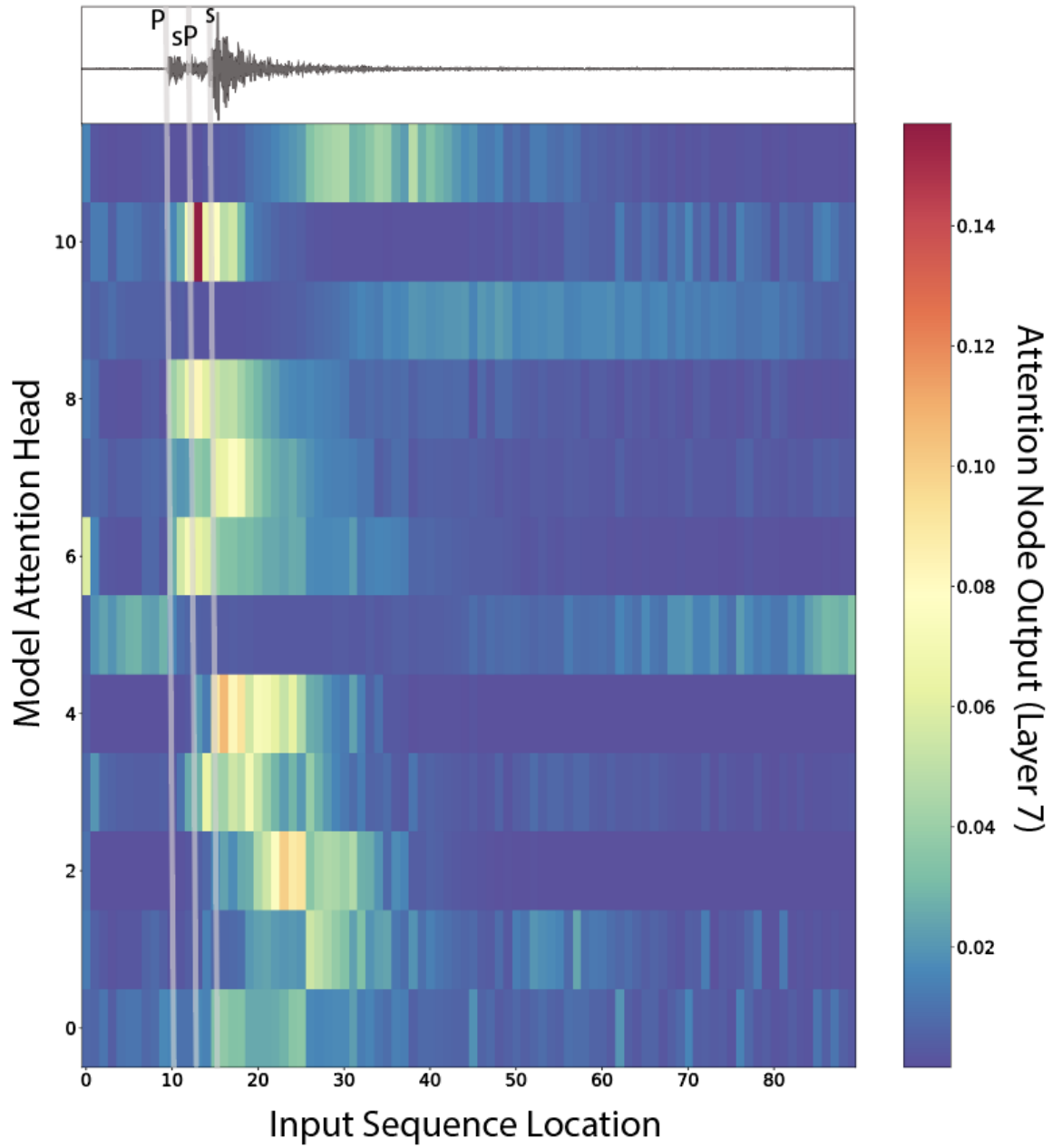
330



331

332

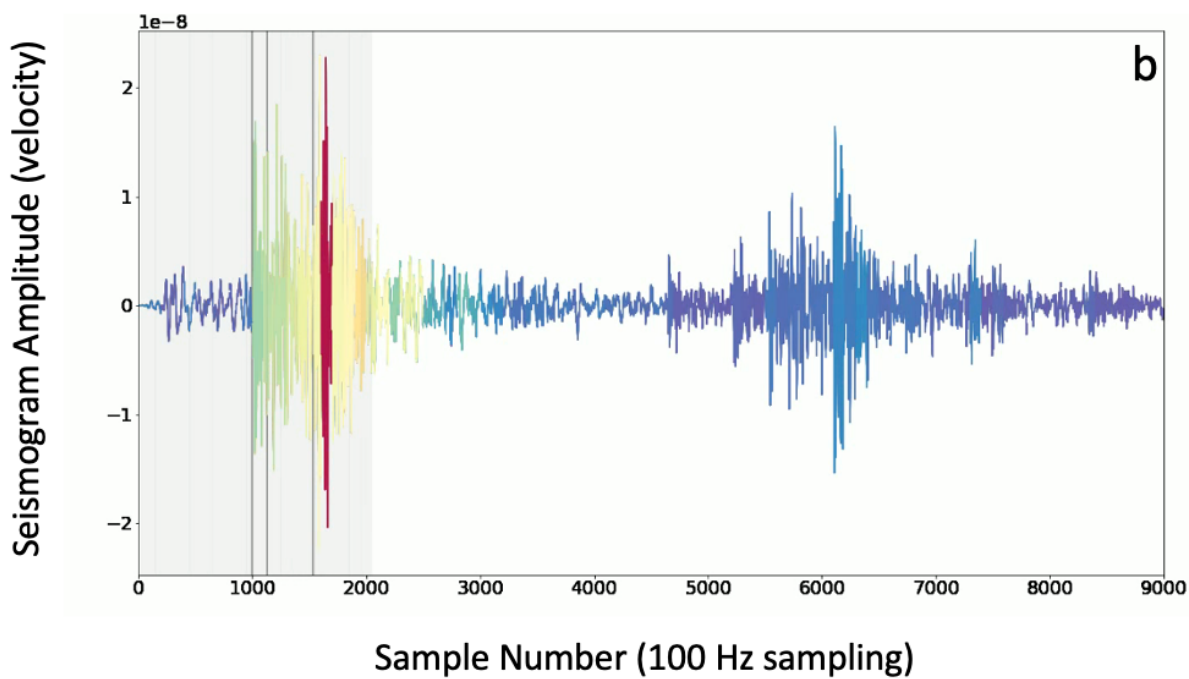
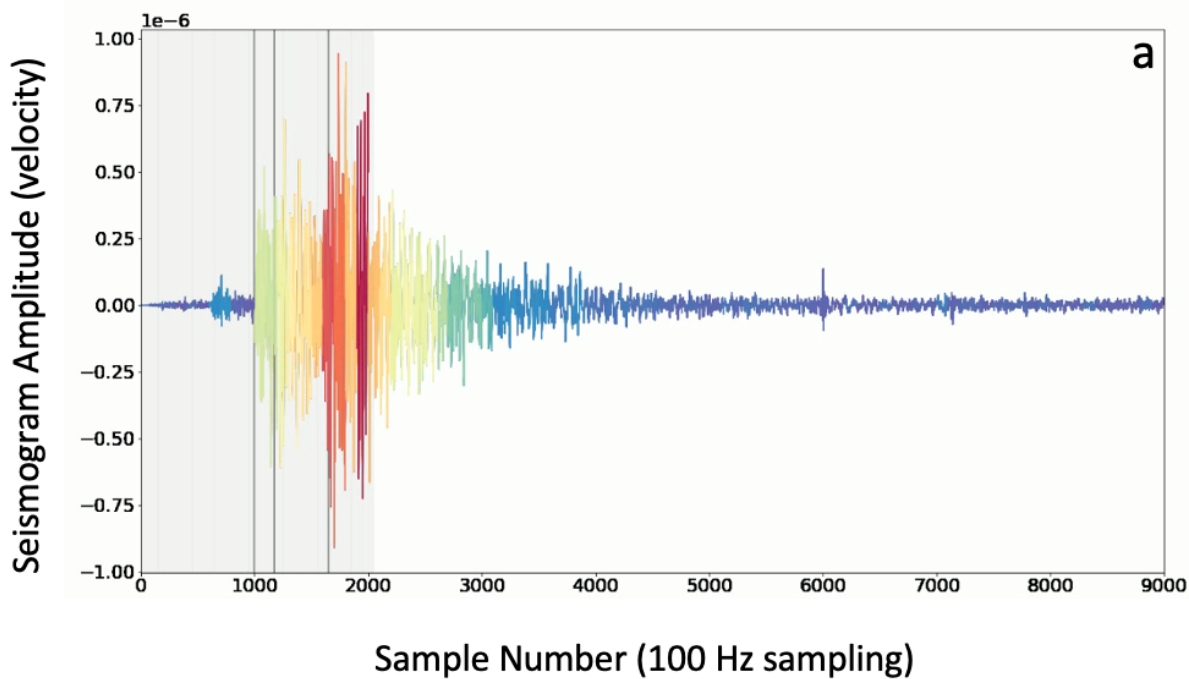
333 *Figure 8. Bidirectional examples of model attention. Input to a layer (bottom) are connected by*  
334 *lines with transparency equivalent to the position and relative strength of attention given to the*  
335 *output sequence (top). The figure panels show which aspects of the temporal sequence are*  
336 *attended to at different locations within the model. For example, the attentions in (a) are nearly*  
337 *equally distributed across the timesteps. Whereas the purple/magenta layer has learned to pay*  
338 *attention to the next value in the sequence. By comparison there are layers where a substantive*  
339 *attention is paid to one location in the output sequence (b), or where discrete outputs are*  
340 *sensitive to surrounding timesteps with receptive fields of various size (c,d,e). Bertviz was used*  
341 *to generate attention views (<https://github.com/jessevig/bertviz>; Vig, 2019)*



342

343 *Figure 9. 12 attention heads for layer 7 responding to the input signal on top at timestep 15.*

344



345  
 346 *Figure 10. Bulk model attention (summed over all layers/heads) for an input signal colored by*  
 347 *relative attention strength (red =high, blue=low). The grey progress bar shows the timestep that*  
 348 *the attention strength is depicting, and the vertical grey lines show calculated body wave arrival*  
 349 *times using TauP and the ak135 velocity model available in the Obspy python library*

350 *(Beyreuther et al.,2010). At timestep 2000 for example, there are discrete segments, perhaps*  
351 *phase arrivals or scattered energy that are most important in making accurate predictions about*  
352 *what the signal should look like at that time.*

## 353 Discussion

354

355 One of the foremost challenges of this work was in deciding the best method of data  
356 preprocessing for representation learning. Power spectral density estimates are compact and  
357 descriptive compared to waveform attributes when the spatio-temporal granularity that results  
358 from the PSD transform is sufficient for the problem. This work discretized PSD estimates at 1  
359 sec resolution into tokens that comprise a seismic vocabulary. Discretization of the PSD  
360 estimates into tokens allowed for the use of existing architectures and training paradigms. The  
361 token sequences (90 tokens per event) without temporal modeling by themselves are only  
362 predictive up to ~81 %. Using random forest at 12-30 tree depths, the differences between test  
363 and train reach a maximum around a tree depth of 30 where train accuracy is above 99% but test  
364 accuracy remains at 81%. Therefore, representation learning and the temporal modeling of the  
365 token sequences both improve learning, although temporal learning plays a larger role than  
366 representation learning based on the difference between fine-tuning results with and without  
367 pretraining (81% with deep RF, 93% with temporal learning, 94.5% with pretraining). For  
368 comparison, binary event prediction on the same dataset can achieve accuracies near the error  
369 rate of this dataset (96-98%) using convolutional architectures. So, while base model training  
370 improves learning, and temporal modeling improves learning substantially, neither are required  
371 for high performance on this task and neither perform as well as other deep learning methods.  
372 While the above findings do not make these models competitive with state-of-the-art in event  
373 discrimination they demonstrate that this method may be excessive if used for the sole learning  
374 problem of binary discrimination when abundant labels are available in a constrained geographic  
375 area.

376

377 This work was meant primarily to prove out that a modeling framework was viable given the  
378 discretization required to utilize NLP ideas developed for language on seismic data. A 1-3%  
379 decrease in overall accuracies on the task of event discrimination is modest compared to the  
380 relatively low competence of non-ML tools for discrimination on the full diversity of events that

381 exist in regional catalogs (specifically for low signal-to-noise ratios; Tibi et al., 2019). If, in  
382 addition to being useful for event discrimination, base models maintain value across multiple  
383 seismic processing tasks and generalized across seismic catalogs or with fewer labels,  
384 substantive benefits could be realized in this domain. Proving that the value of the current  
385 models extends beyond binary event prediction is outside the scope of the current work and  
386 would be an important avenue for continued research.

387

388 The second objective of this work was to begin to use the rich contextual information available  
389 through unlabeled data in exploratory ways. While labeled learning dominates most deep  
390 learning studies in seismic processing, exploratory data analysis with new methods is currently  
391 one of the most underutilized applications in this domain (Mousavi and Beroza, 2022).

392 Exploration of the locus of attention paid to incoming signals suggests that a model's  
393 understanding of an event sequence at any specific time depends on bidirectional context from  
394 the rest of the event. For example, predicting what happens at the end of the event window  
395 depends highly on what happens in the pre-event signal. As you traverse across a signal it is not  
396 simply local bidirectional context but highly specific frames within an event that matter the most.  
397 These may link to meaningful physical phenomena such as discrete phase arrivals or dispersed  
398 energy, or simply express statistically meaningful states for this dataset. Ongoing investigation  
399 may yield valuable insight into the importance these states have on task performance that in the  
400 future lead to simple and powerful predictive models using this new insight.

401

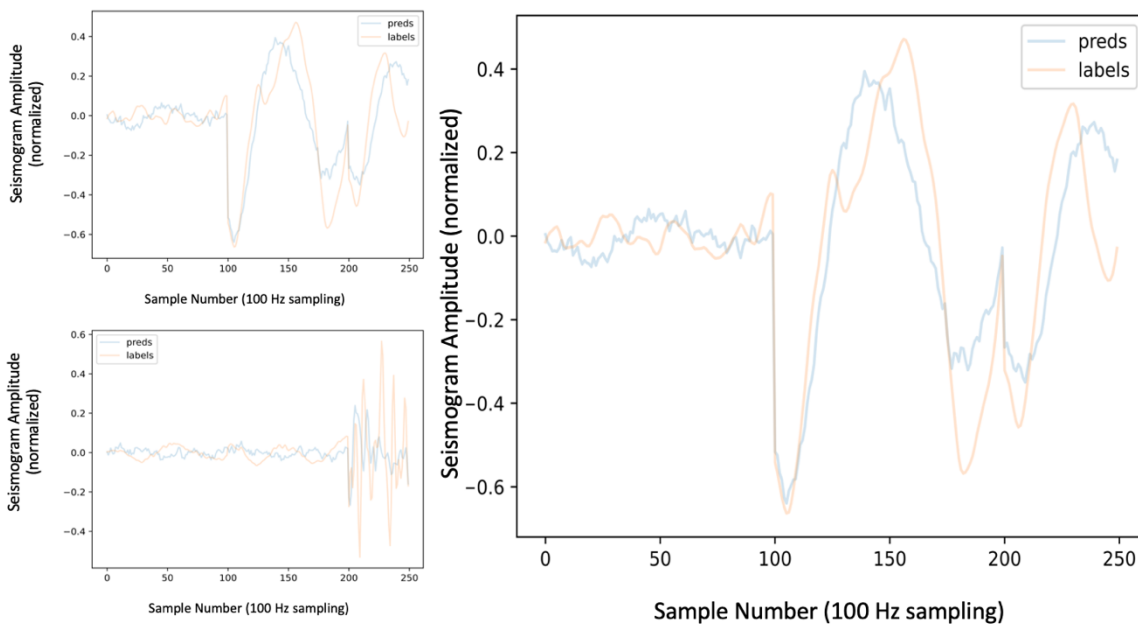
402 Beyond further exploratory work, the value of representations that use bidirectional context  
403 make them an ideal and potentially valuable tool for tasks such as gap filling. Other tasks that  
404 require acausal observations (first arrival picking or earthquake early warning, as examples)  
405 would necessitate alternate training strategies. These open questions and many more remain  
406 targets for future work.

407

408 There are many outstanding computational challenges in self-supervised learning settings with  
409 continuous sensor data. The models tested here required input (batch size) of relatively modest  
410 size when trained on a single GPU (32G memory). While training times also remained modest,  
411 on the order of 1-5 days on a single GPU, parameter optimization was consistently challenging.

412 Many open questions remain regarding the performance ceilings observed here. Advances in  
413 LLM required modeling and data at minimum scales that this work does not approach. It is not  
414 clear if performance in this work was limited by token representations or the need for more and  
415 diverse data, or any number of architecture or search space options that remained unexplored.  
416 Future work may benefit from recent advances in transformer architectures such as Perceiver  
417 networks (Jaegle et al., 2021) which are well suited for NLP style processing without the need  
418 for tokenization and could be a more natural fit for seismic data. A brief trial of a transformer  
419 model’s ability to recreate a seismic waveform for a discrete sample interval (1 sec) was tested  
420 using the perceiver with promising initial results (Figure 11). Future work should focus on  
421 improving learning through scale (dataset and model size) and self-supervised objectives for  
422 richer representation learning in the seismic domain.

423



424  
425 *Figure 11. Waveforms compared to waveform predictions by tokenless transformer*  
426 *architectures. Perceiver models learned to regenerate signals across frequencies of interested*  
427 *but still struggled to recreate random tokens and masked tokens consistently and with high*  
428 *fidelity.*

429  
430 Conclusion

431

432 As we approach ceilings in performance from existing labeled data, self-supervised learning may  
433 be an important tool for utilizing abundant open-source datasets with variable curation legacies  
434 at scale. Base models that are built with self-supervised learning may be important in the  
435 efficient development of a range of models across tasks in a specific domain. Seismic data is  
436 well positioned to take advantage of advancement in the field of self-supervised learning, even  
437 though there are several open questions for the field. Self-supervised learning carries the  
438 additional burden of defining domain appropriate optimization objectives. This work does not  
439 resolve many of the previously unanswered questions about how to exploit seismic data for  
440 better representation learning but it does validate that temporal learning and self-training together  
441 on seismic data result in representations that are physically meaningful and that using those  
442 representation in signal classification achieves better performance than temporal signal modeling  
443 alone.

444

445

446 Acknowledgements

447

448 This Low Yield Nuclear Monitoring (LYNM) research was funded by the National Nuclear  
449 Security Administration, Defense Nuclear Nonproliferation Research and Development (NNSA  
450 DNN R&D). The authors acknowledge important interdisciplinary collaboration with scientists  
451 and engineers from LANL, LLNL, NNSS, PNNL, and SNL. Sandia National Laboratories is a  
452 multimission laboratory managed and operated by National Technology & Engineering Solutions  
453 of Sandia, LLC, a wholly owned subsidiary of Honeywell International Inc., for the U.S.  
454 Department of Energy's National Nuclear Security Administration under contract DE-  
455 NA0003525. The authors acknowledge the support of the National Nuclear Security  
456 Administration Office of Defense Nuclear Nonproliferation Research and Development for  
457 funding this work.

458

459 REFERENCES

460 Beyreuther, M., Barsch, R., Krischer, L., Megies, T., Behr, Y., & Wassermann, J. (2010). ObsPy:  
461 A Python toolbox for seismology. *Seismological Research Letters*, 81(3), 530-533.

462

463 Devlin, J., Chang, M. W., Lee, K., & Toutanova, K. (2018). Bert: Pre-training of deep  
464 bidirectional transformers for language understanding. *arXiv preprint arXiv:1810.04805*.

465

466 Horawalavithana, S., Ayton, E., Sharma, S., Howland, S., Subramanian, M., Vasquez, S.,  
467 Cosbey, R., Glenski, M. and Volkova, S., (2022). Foundation Models of Scientific Knowledge  
468 for Chemistry: Opportunities, Challenges and Lessons Learned.

469

470 Jaegle, A., Borgeaud, S., Alayrac, J. B., Doersch, C., Ionescu, C., Ding, D., ... & Carreira, J.  
471 (2021). Perceiver io: A general architecture for structured inputs & outputs. *arXiv preprint*  
472 *arXiv:2107.14795*.

473

474 Khan, K., Rehman, S. U., Aziz, K., Fong, S., & Sarasvady, S. (2014, February). DBSCAN: Past,  
475 present and future. In *The fifth international conference on the applications of digital*  
476 *information and web technologies (ICADIWT 2014)* (pp. 232-238). IEEE.

477

478 Lacoste, A., Sherwin, E. D., Kerner, H., Alemohammad, H., Lütjens, B., Irvin, J., ... & Vazquez,  
479 D. (2021). Toward Foundation Models for Earth Monitoring: Proposal for a Climate Change  
480 Benchmark. *arXiv preprint arXiv:2112.00570*.

481

482 Le, N. Q. K., Ho, Q. T., Nguyen, T. T. D., & Ou, Y. Y. (2021). A transformer architecture based  
483 on BERT and 2D convolutional neural network to identify DNA enhancers from sequence  
484 information. *Briefings in bioinformatics*, 22(5), bbab005.

485

486 Linville, L., Pankow, K., & Draelos, T. (2019). Deep learning models augment analyst decisions  
487 for event discrimination. *Geophysical Research Letters*, 46(7), 3643-3651.

488

489 Linville, L. M. (2022). Event-Based Training in Label-Limited Regimes. *Journal of Geophysical*  
490 *Research: Solid Earth*, 127(1), e2021JB022820.

491

492 McInnes, L., Healy, J., & Melville, J. (2018). Umap: Uniform manifold approximation and  
493 projection for dimension reduction. *arXiv preprint arXiv:1802.03426*.

494

495 Mikolov, T., Grave, E., Bojanowski, P., Puhersch, C., & Joulin, A. (2017). Advances in pre-  
496 training distributed word representations. *arXiv preprint arXiv:1712.09405*.

497

498 Mousavi, S. M., & Beroza, G. C. (2022). Deep-learning seismology. *Science*, 377(6607),  
499 eabm4470.

500

501 Narkhede, M. V., Bartakke, P. P., & Sutaone, M. S. (2022). A review on weight initialization  
502 strategies for neural networks. *Artificial intelligence review*, 55(1), 291-322.

503

504 Pedregosa, F., Varoquaux, G., Gramfort, A., Michel, V., Thirion, B., Grisel, O., ... & Duchesnay,  
505 E. (2011). Scikit-learn: Machine learning in Python. *the Journal of machine Learning research*,  
506 12, 2825-2830.

507

508 Rudin, C. (2019). Stop explaining black box machine learning models for high stakes decisions  
509 and use interpretable models instead. *Nature Machine Intelligence*, 1(5), 206-215.

510

511 Steinley, D. (2006). K-means clustering: a half-century synthesis. *British Journal of*  
512 *Mathematical and Statistical Psychology*, 59(1), 1-34.

513

514 Tibi, R., Linville, L., Young, C., & Brogan, R. (2019). Classification of Local Seismic Events in  
515 the Utah Region: A Comparison of Amplitude Ratio Methods with a Spectrogram-Based  
516 Machine Learning Approach Classification of Local Seismic Events in the Utah Region. *Bulletin*  
517 *of the Seismological Society of America*, 109(6), 2532-2544.

518

519 Vaswani, A., Shazeer, N., Parmar, N., Uszkoreit, J., Jones, L., Gomez, A. N., ... & Polosukhin, I.  
520 (2017). Attention is all you need. *Advances in neural information processing systems*, 30.

521

522 Vig, J. (2019). A multiscale visualization of attention in the transformer model. *arXiv preprint*  
523 *arXiv:1906.05714*.

524

525

526

527